Human Molecular Genetics, 2011, Vol. 20, No. 8 ***1574–1584***
doi:10.1093/hmg/ddr034
Advance Access published on January 27, 2011

Impairment of the tRNA-splicing endonuclease subunit 54 (*tsen54*) gene causes neurological abnormalities and larval death in zebrafish models of pontocerebellar hypoplasia

Paul R. Kasher[1], Yasmin Namavar[1], Paula van Tijn[4,7], Kees Fluiter[1], Aleksander Sizarov[2], Maarten Kamermans[5], Andrew J. Grierson[6], Danica Zivkovic[7] and Frank Baas[1,3,*]

[1]Department of Genome Analysis, [2]Heart Failure Research Centre and [3]Department of Neurology, Academic Medical Center, Meibergdreef 9, 1105AZ Amsterdam, The Netherlands, [4]Department of Astrocyte Biology and Neurodegeneration and [5]Research Unit Retinal Signal Processing, Netherlands Institute for Neuroscience, Royal Netherlands Academy of Arts and Sciences, Meibergdreef 47, 1105BA Amsterdam, The Netherlands, [6]Department of Neuroscience, The Sheffield Institute for Translational Neuroscience, University of Sheffield, 385A Glossop Road, S10 2HQ, UK and [7]Hubrecht Institute for Developmental Biology and Stem Cell Research, Royal Netherlands Academy of Arts and Sciences and University Medical Center Utrecht, Uppsalalaan 8, 3548CT Utrecht, The Netherlands

Received December 6, 2010; Revised January 21, 2011; Accepted January 22, 2011

Pontocerebellar hypoplasia (PCH) represents a group (PCH1–6) of neurodegenerative autosomal recessive disorders characterized by hypoplasia and/or atrophy of the cerebellum, hypoplasia of the ventral pons, progressive microcephaly and variable neocortical atrophy. The majority of PCH2 and PCH4 cases are caused by mutations in the *TSEN54* gene; one of the four subunits comprising the tRNA-splicing endonuclease (TSEN) complex. We hypothesized that *TSEN54* mutations act through a loss of function mechanism. At 8 weeks of gestation, human *TSEN54* is expressed ubiquitously in the brain, yet strong expression is seen within the telencephalon and metencephalon. Comparable expression patterns for *tsen54* are observed in zebrafish embryos. Morpholino (MO) knockdown of *tsen54* in zebrafish embryos results in loss of structural definition in the brain. This phenotype was partially rescued by co-injecting the MO with human *TSEN54* mRNA. A developmental patterning defect was not associated with *tsen54* knockdown; however, an increase in cell death within the brain was observed, thus bearing resemblance to PCH pathophysiology. Additionally, *N*-methyl-*N*-nitrosourea mutant zebrafish homozygous for a *tsen54* premature stop-codon mutation die within 9 days post-fertilization. To determine whether a common disease pathway exists between *TSEN54* and other PCH-related genes, we also monitored the effects of mitochondrial arginyl-tRNA synthetase (*rars2*; PCH1 and PCH6) knockdown in zebrafish. Comparable brain phenotypes were observed following the inhibition of both genes. These data strongly support the hypothesis that *TSEN54* mutations cause PCH through a loss of function mechanism. Also we suggest that a common disease pathway may exist between *TSEN54*- and *RARS2*-related PCH, which may involve a tRNA processing-related mechanism.

INTRODUCTION

Pontocerebellar hypoplasia (PCH) represents a group of neurodegenerative autosomal recessive disorders characterized by severe mental and motor impairments. The disease is associated with prenatal onset, hypoplasia/atrophy of the cerebellum, hypoplasia of the ventral pons, progressive microcephaly and variable neocortical atrophy. The median life expectancy is

*To whom correspondence should be addressed at: Department of Genome Analysis, Academic Medical Center, Meibergdreef 9, 1105AZ Amsterdam, The Netherlands. Tel: +31 205663846; Fax: +31 205669312; Email: f.baas@amc.uva.nl

50 months (1); however, in rare cases, the most severe forms can lead to fatality during early post-natal periods. To date, six subtypes of PCH (PCH1–6) have been distinguished based on varying clinical and pathological features (1–6).

Mutations in three of the four subunit genes comprising the tRNA-splicing endonuclease (TSEN) complex are responsible for PCH2 and PCH4 (1,2). The TSEN complex is a heterotetramic enzyme comprised of two structural subunits, TSEN54 and TSEN15, and two catalytic subunits, TSEN2 and TSEN34 (7,8). Mutations in the *TSEN54* subunit gene are the most frequent cause of PCH2 and PCH4, and a common mutation (p.A307S) has been identified in the majority of patients. A homozygous p.A307S mutation is strongly associated with a PCH2 phenotype. The p.A307S mutation occurring compound heterozygous with a *TSEN54* null allele is associated with a severe PCH4 phenotype (1). Other less common *TSEN54* mutations, as well as rare mutations occurring in the *TSEN2* and *TSEN34* subunit genes have also been identified in PCH2 and PCH4 cases (1,2).

tRNAs play an essential role in protein synthesis where the anticodon of a mature tRNA molecule recognizes and interacts with the codon displayed by the mRNA. Through the activity of the ribosome, this process allows condensation of the tRNA-specific amino acid with the peptide chain on the adjacent tRNA (9). Part of the maturation process is the removal of an intronic sequence that exists within the anticodon loop of some tRNA genes. Splicing of the intron is performed through a composite active site of the TSEN complex (8). In humans, only 6.2% of tRNA genes contain an intron and therefore require TSEN function for maturation and exposure of the anticodon, necessary for downstream translation. Multiple genes exist for each tRNA and in some circumstances the vast majority or all tRNA genes for a particular codon are intron-containing. For example, in humans, 13 of the 14 genes encoding $tRNA^{Tyr}$-(GTA) contain an intron. Therefore, a defective TSEN complex is likely to lead to a shortage of tRNA tyrosine. Other examples exist including $tRNA^{Ile}$-(TAT), $tRNA^{Leu}$-(CAA) and $tRNA^{Arg}$-(TCT). More details can be viewed at http://lowelab.ucsc.edu/GtRNAdb/.

In most cases, PCH4 patients, who are more severely affected than PCH2 patients, have a null allele and a missense mutation in the *TSEN54* subunit gene (1). This genotype–phenotype observation supports a hypothesis for a loss of TSEN function in PCH2 and PCH4 pathophysiology. The TSEN complex is not only involved in tRNA splicing. It also plays a role in mRNA 3′ end formation (7). Therefore, it is possible that other functions of the TSEN complex may play a role in the disease pathogenesis of PCH2 and PCH4 cases.

How mutations in a gene involved with tRNA splicing and protein synthesis can lead to a brain-specific defect is unclear. *TSEN54* is expressed throughout the body; however, there are differences in expression levels between various tissues (http://www.genecards.org/cgi-bin/carddisp.pl?gene=TSEN54&search=tsen54). Strong *TSEN54* mRNA expression has been observed in neuronal populations in the developing cerebellum, pons and olivary nuclei at 23 weeks of gestation (2). This and the selective degeneration in PCH could suggest that TSEN activity is required at high levels in the brain structures affected in the disease. At 23 weeks of gestation, the brain has already significantly increased in volume and is well established neuroanatomically (10). Neonatal ultrasound analysis in PCH2 patients reveals that the cerebellum develops as normal to gestation week 29; however, from gestation week 31, cerebellar hypoplasia can be observed (11). In addition, cell death in the pons has been reported in PCH patients at low levels following pathological examination (5). It is likely that high levels of degeneration are present during the time course of disease; however, most cells will have degenerated at the time of death and are thus unavailable for post-mortem analysis.

As PCH is a rare and lethal neurodegenerative disorder, patient material is scarce. To further understand the role of TSEN in the pathophysiology of PCH, a disease model is required. Zebrafish are now a well-established tool used to model various neurodegenerative disorders (12). In this current study, we have utilized two separate genetic approaches to produce zebrafish models of *TSEN54*-related PCH. These include an antisense morpholino (MO) oligonucleotide-induced knockdown of *tsen54* and also an *N*-methyl-*N*-nitrosourea (ENU) mutagenesis strategy to produce a zebrafish strain harbouring a *tsen54* premature stop-codon mutation. Here, we show that the knockdown of *tsen54* results in brain hypoplasia and loss of structural definition in the brain, which is associated with increased cell death but not a developmental patterning defect, whereas genetic knockout of *tsen54* is lethal. Additionally, the knockdown of the mitochondrial arginyl-tRNA synthetase (*rars2*) gene, (*RARS2* mutations cause PCH1 and PCH6) (1,4,13) results in a phenotype that is comparable with *tsen54* depletion. Using these novel disease models of PCH, we provide the first evidence in an experimental model that *TSEN54* mutations act through a loss of function mechanism and that a common disease pathway may exist between PCH subtypes due to either *TSEN54* or *RARS2* mutations.

RESULTS

TSEN54 expression during early development in human and zebrafish

To examine *TSEN54* expression during early brain development, we performed *in situ* hybridization on 8-week-old human fetal brain sections using *TSEN54*-specific locked nucleic acid/2′-O-methyl RNA (LNA/2OME) probes. *TSEN54* mRNA is expressed throughout the brain at this early stage, with high levels of expression observed within the developing telencephalon and metencephalon (Fig. 1A). During normal development, the metencephalon later forms the pons and cerebellum (14). Analysis of other tissues shows relatively high *TSEN54* expression in spinal cord and liver, whereas expression in other tissues was low (Supplementary Material, Fig. S1). We next examined the expression pattern of zebrafish *tsen54* in embryos at 24 h post-fertilization (hpf). The zebrafish *TSEN54* orthologue (also known as zgc: 109927; accession number: NM_001020529) shares 46% identity to the human gene. As shown in Figure 1B, *tsen54* expression is ubiquitous, with strong expression in the brain within the telencephalon and mid-hindbrain boundary (MHB). *tsen54* is also expressed ubiquitously during early embryogenesis in zebrafish as observed from the 8-cell stage to the somite stages (Supplementary Material, Fig. S2).

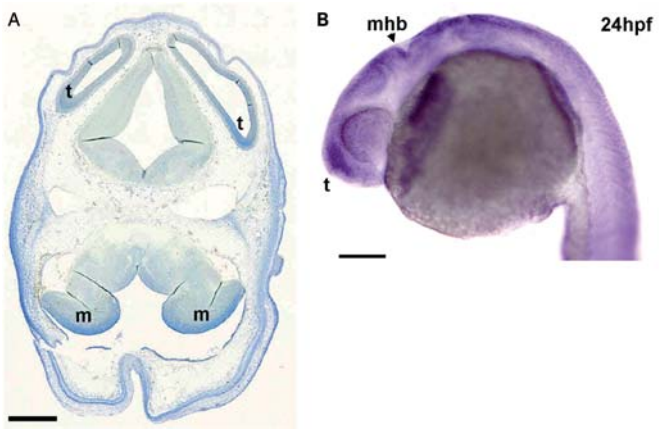

Figure 1. *TSEN54* expression is ubiquitous but strong in the brain in human and zebrafish during early stages of neurodevelopment. (**A**) *TSEN54 in situ* hybridization within transverse section of a human foetal brain at 8 weeks prenatal age. *TSEN54* mRNA is widely expressed throughout brain and head tissue, but strongly expressed in the developing metencephalon (m) and telencephalon (t). Scale bar = 1 mm. (**B**) Lateral view of *tsen54* whole-mount *in situ* hybridization in zebrafish embryo. Ubiquitous *tsen54* mRNA expression pattern is observed at 24 hpf in zebrafish embryos, with strongest expression observed within the brain, especially the telencephalon (t) and mid-hindbrain boundary (mhb). Scale bar = 200 μm.

MO knockdown of *tsen54* causes loss of structural integrity in the zebrafish brain

As TSEN54-related PCH is inherited in an autosomal recessive manner, the biological mechanism underlying the disease is likely to be associated with a loss of TSEN54 function. To test this hypothesis in a model system, we were interested in monitoring the effects of knocking down the zebrafish *tsen54* gene using an antisense MO oligonucleotide approach. In comparison to wild-type (WT) un-injected (Fig. 2A) and control MO (CoMO)-injected embryos (Fig. 2B) at 24 hpf, injection of 2.5 ng *tsen54* translation blocking (ATG) MO (Fig. 2C) resulted in abnormalities within the head including brain hypoplasia and loss of structural integrity inside the brain. Clear structural definition of the MHB (denoted by an asterisk) was apparent in the control embryos (Fig. 2A and B); however, this structure appeared aberrant in *tsen54* morphants (Fig. 2C and D). In zebrafish embryos, the MHB is a key structure involved with the neuronal migration and the development of the cerebellum (15). To exclude the possibility that the effect was due to a non-specific effect and to confirm specific targeting of the MO (16), we designed a second *tsen54* MO that targeted the exon 8 splice donor site of the *tsen54* gene. As shown in Figure 2D, we observe comparable brain hypoplasia and reduced structural definition in splice-site morphants. Reverse transcriptase–polymerase chain reaction (RT–PCR) of cDNA synthesized from WT, CoMO and splice-site morphant embryos confirmed abnormal splicing of the *tsen54* gene in the morphants (Fig. 2G). To further confirm that the phenotype was directly attributable to the knockdown of *tsen54*, we attempted to rescue the brain phenotype associated with *tsen54* depletion by co-injecting the ATG MO with human *TSEN54* mRNA. As shown in Figure 2E, injection of 233 pg human *TSEN54* mRNA alone produced no effects upon brain structure. Co-injection of *tsen54* ATG MO and human *TSEN54* mRNA resulted in a partial rescue of the brain phenotype observed with MO only (Fig. 2F). Co-injected embryos display generally milder brain hypoplasia and more clearly defined brain structure when compared with ATG alone (Fig. 2C). We next quantified the proportion of brain phenotypes associated with each treatment at 24 hpf (Fig. 2H). Brain phenotypes were classified as either normal (appeared as WT), mild (slight brain hypoplasia, slight reduction in structural definition in the brain) or severe (severe brain hypoplasia, complete loss of brain structural definition). As expected, predominantly normal brain phenotypes were associated with both control groups (WT un-injected, human *TSEN54* mRNA only). Knockdown of *tsen54* with the ATG MO was associated with a mostly severe brain phenotype (76%), although mild (13%) and normal (11%) brain phenotypes were also observed to a lesser extent. Co-injection of the ATG MO with human *TSEN54* mRNA resulted in a striking reduction in the proportion of embryos displaying a severe brain phenotype (8%) and a shift to a predominantly mild (67%) brain phenotype. Indeed, the percentage of normal brain phenotypes also increased (25%) within the rescue group. Therefore, human *TSEN54* is capable of partially rescuing the brain phenotype associated with the loss of *tsen54* translation, thus confirming specific targeting of the MO.

Inhibition of *tsen54* translation produces a brain defect which is not associated with a developmental patterning deficiency

PCH is characterized by hypoplasia and atrophy of the cerebellar hemispheres, hypoplasia of the pons and a general delay of neurodevelopment (17). To determine whether the brain phenotype caused by *tsen54* knockdown in zebrafish embryos was associated with a developmental brain patterning defect, we performed *in situ* hybridization on whole-mount embryos at 24 hpf using *fgf8* (*fibroblast growth factor 8*) and *otx2* (*orthodenticle homeobox 2*) RNA probes as markers of brain development. In zebrafish brain, *Fgf8* is expressed in the MHB and plays a role in the maintenance and development of this region, which includes the cerebellum (18). In addition, *Fgf8* is also expressed within the telencephalon and optic vesicles (19). *Otx2* plays a role in early regionalization of the mesencephalon and indeed is expressed within fore-midbrain regions during early development in zebrafish (20). Abnormal localization of the expression of these genes within morphants would suggest a defect in the developmental patterning of these brain regions. As shown in Figure 3A, embryos injected with human *TSEN54* mRNA alone show normal expression patterning of *Fgf8*. When the brain was observed from a dorsal perspective (Fig. 3D), the expression of *Fgf8* appeared as a ‘horseshoe with a peak’ pattern in control embryos. MO knockdown of *tsen54* was not associated with abnormal patterning (Fig. 3B), as *Fgf8* expression was correctly observed within the MHB and telencephalon. However, compared with controls, the MHB appeared compressed, thus reflecting the brain hypoplasia associated with *tsen54* knockdown. This result is further supported when observing the dorsal view of the morphant brain where the ‘peak’ of the ‘horseshoe’ was absent from the MHB (Fig. 3E, arrow). Loss of this horseshoe peak was reversed, to a certain extent, by co-injecting the *tsen54* ATG MO with human *TSEN54*

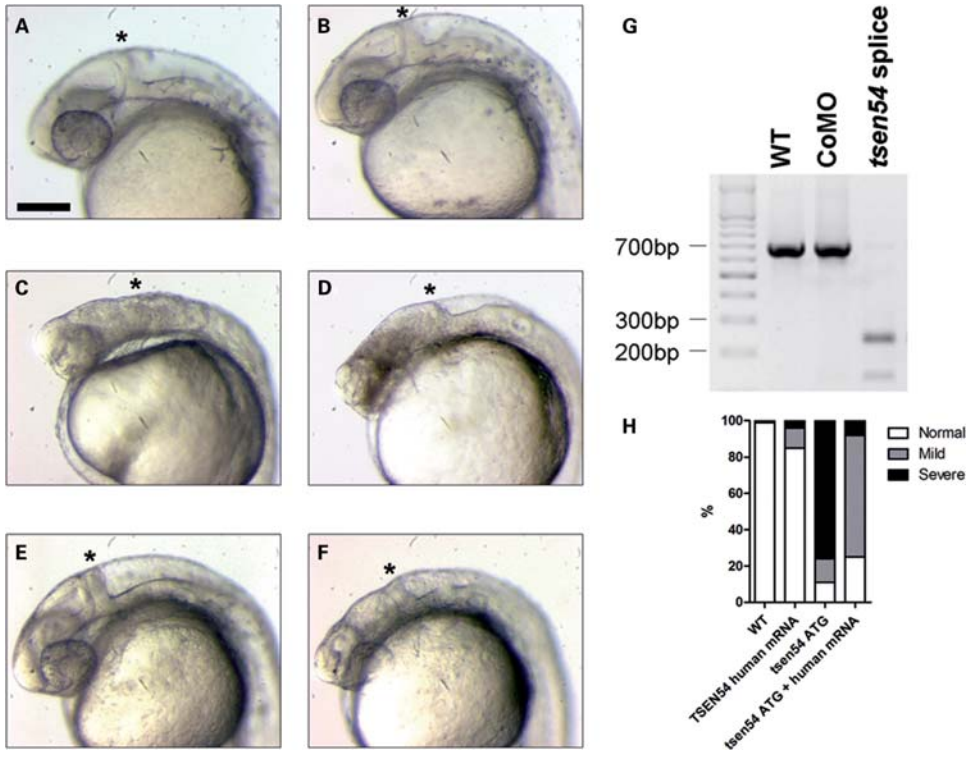

Figure 2. Disruption of *tsen54* translation causes brain hypoplasia and loss of structural definition in the MHB in zebrafish embryos. (**A**–**F**) Lateral views of head and brain regions of *tsen54* MO and human *TSEN54* mRNA-injected zebrafish embryos at 24 hpf. Asterisks denote the MHB. (A) WT un-injected embryo; (B) CoMO-injected embryo; (C) *tsen54* ATG MO-injected embryo; (D) *tsen54* exon 8 splice donor site MO-injected embryo; (E) human *TSEN54* mRNA-injected embryo; (F) rescued embryo co-injected with *tsen54* ATG MO and human *TSEN54* mRNA. Scale bar = 200 μm. (**G**) RT–PCR using primers located in exons 7 and 10 in *tsen54* cDNA synthesized from RNA extractions from WT un-injected embryos, CoMO-injected embryos and *tsen54* exon 8 splice donor site MO-injected embryos. RT–PCR using samples from control embryos produced a band of 696 bp in length. Shorter products observed in splice MO-injected embryos indicate abnormal splicing of the *tsen54* gene. (**H**) Quantification of phenotypes observed in WT un-injected embryos, human *TSEN54* mRNA-injected embryos, *tsen54* ATG MO-injected embryos and rescued embryos co-injected with ATG MO and human mRNA. For each group, 50–100 embryos were analysed. Embryos were classified as displaying normal (white), mild (grey) or severe (black) phenotypes. There is a shift from a predominantly severe phenotype in the *tsen54* ATG MO group to a predominantly mild phenotype in ATG MO and human *TSEN54* mRNA co-injection group, thus illustrating the partial rescue of the brain phenotype associated with the loss of *tsen54*.

mRNA, further confirming specific gene targeting (Fig. 3C and F). Similarly, *tsen54* knockdown did not result in abnormal patterning of the fore-midbrain as localization of *Otx2* expression was comparable between morphants (Fig. 3H) and controls (Fig. 3G). However, the brain hypoplasia phenotype was further illustrated by the reduction in intensity and extent of the *Otx2* expression pattern in morphants compared with controls (Fig. 3J and K), which could be partially rescued by the introduction of human *TSEN54* mRNA (Fig. 3I and L).

Brain phenotype caused by *tsen54* knockdown is associated with increased cell death

As the brain phenotype caused by *tsen54* knockdown was not associated with a neurodevelopmental patterning defect, we next monitored the levels of neurodegeneration in the brains of morphant embryos. Embryos were incubated with acridine orange, a vital dye that binds to nucleic acids in damaged cells (21). The numbers of fluorescing cells within the brain were counted from 10 to 20 embryos per group (at 24 hpf). Low numbers of fluorescing cells were counted in the brains of WT embryos (Fig. 4A and E; 55.5 ± 4; mean ± SEM) and *TSEN54* mRNA-injected embryos (Fig. 4B and E; 80.7 ± 7). In comparison to both of the control groups, injection of the *tsen54* ATG MO resulted in a significant increase in the number of fluorescing cells within the brain (Fig. 4C and E; 242.9 ± 16; $P < 0.0001$). Co-injection of *tsen54* ATG MO with human *TSEN54* mRNA resulted in a significant reduction in the numbers of fluorescing cells in comparison to the *tsen54* ATG injection only group (Fig. 4D and E; 173.9 ± 7.8; $P = 0.0005$); however, the number of fluorescing cells in this group was still significantly greater than that of both control groups ($P < 0.0001$). Therefore, this result further confirms that human *TSEN54* is capable of partially rescuing the brain phenotype associated with *tsen54* knockdown.

A homozygous premature stop-codon mutation within *tsen54* causes early lethality in zebrafish

Antisense MO oligonucleotides allow a highly efficient means of knocking down gene function during early embryonic development; however, the effects diminish after a few days post-fertilization (dpf) (12). Therefore, we generated a stable zebrafish model that harboured a mutation within the *tsen54* gene in order to study the survival rates. We screened the

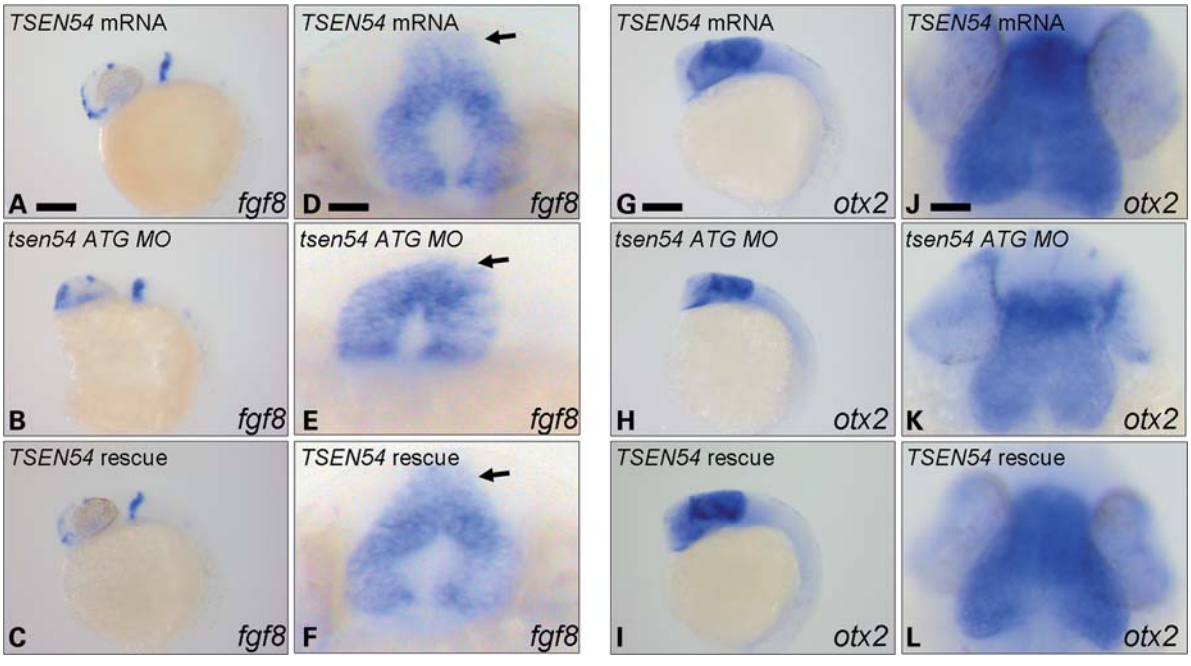

Figure 3. Knockdown of zebrafish *tsen54* results in a brain defect that is not associated with abnormal developmental patterning. Whole-mount *in situ* hybridization using *fgf8* (**A**–**F**) and *otx2* (**G**–**L**) DIG RNA probes in 24 hpf embryos injected with human *TSEN54* mRNA alone (A, D, G and J), *tsen54* ATG MO (B, E, H and K) and *tsen54* ATG MO with human *TSEN54* mRNA rescue (C, F, I and L). Lateral views are presented in (A)–(C) for *fgf8* staining and (G)–(I) for *otx2* staining (scale bar = 200 μm). Dorsal views are presented in (D)–(F) for *fgf8* staining (scale bar = 30 μm) and (J)–(L) for *otx2* staining (scale bar = 50 μm). Results reveal brain hypoplasia is evident in *tsen54* morphants, as indicated by the loss of the *fgf8* 'horseshoe peak' expression pattern (arrows) however, developmental patterning of the MHB (*fgf8*) and fore-midbrain (*otx2*) are normal. Co-injection of the ATG MO with *TSEN54* human mRNA is capable of partially rescuing the brain hypoplasia phenotype, thus confirming specific targeting of the MO.

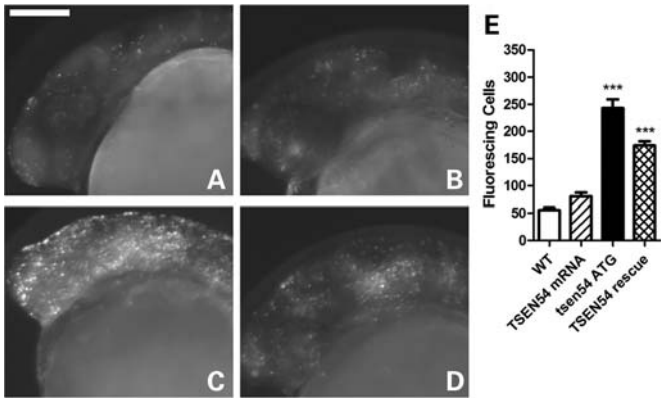

Figure 4. *tsen54* knockdown is associated with increased cell death in the brain. (**A**–**D**) Lateral view of brains of live zebrafish embryos (24 hpf) incubated with acridine orange in WT un-injected (A), human *TSEN54* mRNA alone (B), *tsen54* ATG MO (C) and *tsen54* ATG MO co-injected with human *TSEN54* mRNA rescue (D) groups. Scale bar = 200 μm. (**E**) Quantification of fluorescing cells from each group ($n = 10$–20). Dead cells were counted from the tip of the forebrain to the ear, excluding the eye. Injection of *tsen54* ATG MO resulted in a significant increase in the number of dead cells within the brain. Co-injection of the ATG MO with human *TSEN54* mRNA resulted in a significant decrease in cell death ($^{***}P < 0.0005$).

zebrafish ENU mutagenesis DNA archive at the Hubrecht Laboratories, Utrecht (22), and identified a heterozygous C > T substitution in exon 8 of the *tsen54* gene (c.682C > T; Fig. 5A). The position of this mutation translates as the conversion of an arginine to a premature stop codon at amino acid position 228 (p.R228X). Heterozygotes from the F2 progeny were identified by genotyping and the mutation was backcrossed onto a WT AB background for five generations to reduce the number of potentially confounding ENU mutations (23). All mutants from this breeding programme were subsequently referred to as *tsen54*^{R228X}. As PCH is an autosomal recessive disease, we next performed an in-cross between heterozygous mutants to test for homozygosity. Embryos resulting from the in-cross were genotyped at 1, 2 and 3 weeks post-fertilization. All three genotypes were present after 1 week; however, at 2 weeks post-fertilization, *tsen54*$^{R228X-/-}$ animals were absent, suggesting that homozygosity was lethal during the larval stages (data not shown). To determine the precise time point at which the lethality of *tsen54*$^{R228X-/-}$ larvae occurred, we performed a survival analysis. As shown in Fig. 5B, larvae obtained from a control WT TL in-cross showed 72% survival after 3 weeks, whereas only 45% of the *tsen54*$^{R228X+/+}$ embryos survived to 21 dpf, probably due to the retention of an ENU mutation on the *tsen54*$^{R228X+/+}$ background. Of the *tsen54*$^{R228X+/-}$ heterozygous embryos, 62% survived to 21 dpf. Confirming our observations on the lethality of homozygosity for the mutation, all *tsen54*$^{R228X-/-}$ larvae had died by 9 dpf (Fig. 5B).

Disruption of the *rars2* gene results in a brain phenotype comparable with *tsen54* morphants

Mutations in the nuclear-encoded *RARS2* gene are found in PCH1 and PCH6 (1,4,13). RARS2 plays a role in the

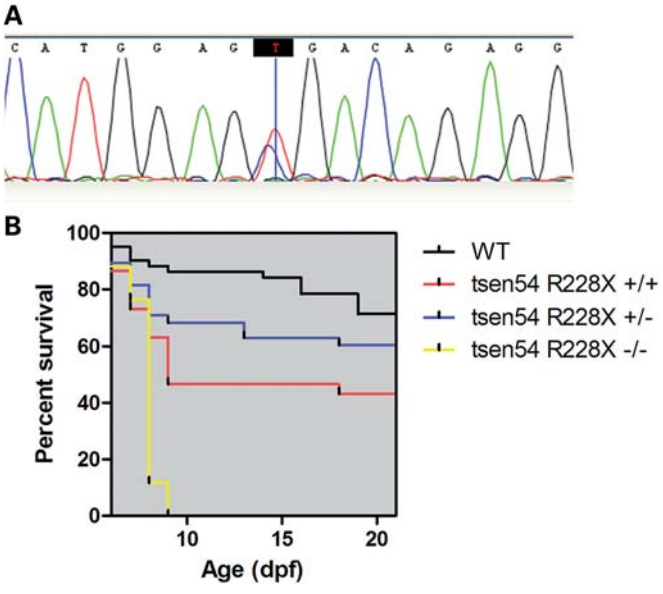

Figure 5. A homozygous premature stop-codon mutation within *tsen54* causes early lethality in zebrafish larvae. (**A**) Sequence trace obtained from the individual heterozygous c.682C > T *tsen54* mutant (hu5985). Translation of this base pair substitution leads to the p.R228X mutation. The mutation was subsequently backcrossed onto a WT background for five generations. (**B**) Progeny from a *tsen54*$^{R228X+/-}$ in-cross were observed for 3 weeks post-fertilization to test for homozygosity. Survival was plotted using the Kaplan–Meier curves. By 9 dpf, 100% of the *tsen54*$^{R228X-/-}$ (yellow line) larvae had died. In comparison, 45% and 62% of the *tsen54*$^{R228X+/+}$ (red line) and *tsen54*$^{R228X+/-}$ (blue line) survived to the 3 weeks post-fertilization time point, respectively. As a comparison to general ENU mutant survival, 72% WT TL larvae (black line) were observed to survive to the 21 dpf stage.

aminoacylation of mitochondrial tRNA^{Arg} (4). Thus, a common disease mechanism related to tRNA processing may account for different PCH subtypes caused by mutations in *TSEN54* or *RARS2*. Similar to *tsen54*, *rars2* is expressed ubiquitously at 24 hpf but strong within the head and brain (24). To test the effects of *rars2* inhibition, we injected zebrafish embryos with MOs designed to target the *rars2* ATG start site and the exon 6 splice donor site. As shown in Figure 6C and D, knockdown of *rars2* with both MOs results in brain hypoplasia and loss of structural definition within the brain in comparison to control embryos (Fig. 6A and B). RT–PCR reveals that abnormal splicing of *rars2* occurred in the splice-site morphants (Fig. 6G). Co-injection of human *RARS2* mRNA with the *rars2* ATG MO resulted in partial recovery of the brain phenotype, thus confirming specific targeting of gene knockdown (Fig. 6E, F and H). Whole-mount *in situ* hybridization using *fgf8* (Supplementary Material, Fig. S3A–F) and *otx2* (Supplementary Material, Fig. S3G–L) RNA probes further illustrates the brain hypoplasia phenotype observed in *rars2* morphants. Similar to *tsen54* knockdown, developmental patterning of the MHB and the fore-midbrain regions was not affected. Furthermore, *rars2* knockdown was associated with a significant increase in cell death within the brains of morphant embryos (Supplementary Material, Fig. S4C and E) when compared with both control groups ($P < 0.0001$; Supplementary Material, Fig. S4A, B and E). The number of dead cells was significantly reduced when human *RARS2* mRNA was co-injected with the *rars2* ATG MO ($P = 0.0005$; Supplementary Material, Fig. S4D and E). Taken together, these observations reveal phenotypic comparisons between *rars2* and *tsen54* morphants, suggesting a common disease pathway may exist between two separate genes in the pathogenesis of distinct subtypes of PCH.

DISCUSSION

In this study, we show that the inhibition of *tsen54* in zebrafish leads to neurological abnormalities and is lethal, thus bearing similarities to the disease characteristics associated with PCH. In addition, these data strongly support the hypothesis that *TSEN54* mutations cause the disease through a loss of function mechanism. A strong and specific expression pattern for *TSEN54* in developing human cerebellar neurons at gestation week 23 has been reported previously (2). Here, we show that *TSEN54* mRNA is ubiquitously expressed in the brain at 8 weeks of development with strong expression observed within the developing metencephalon and telencephalon. The metencephalonic region of the developing brain eventually forms the pons and cerebellum (25). Abnormalities in both of these regions are the hallmark features of PCH pathology as all six subtypes of PCH are characterized by hypoplasia and variable atrophy of the cerebellum and pons (1–6). The telencephalon gives rise to the cerebral cortex and basal ganglia within the cerebral hemispheres (26). Cerebral cortical atrophy has been reported in 40% of *TSEN54*-related PCH patients, a feature that correlates with increasing age, suggesting all patients would display such a phenotype if survival rates were higher (1). Cerebral immaturity is also a key feature for PCH4 diagnosis (1). Also, although less common, microglial and astrocytic pathology have also been reported in the basal ganglia in PCH2 (17). Therefore, strong *TSEN54* expression is apparent in those brain regions affected in PCH during the earlier stages of neurodevelopment. In zebrafish, we observed a ubiquitous expression pattern of *tsen54*; however, strongest expression was detected within the brain at 24 hpf, in particular the telencephalon and MHB. Ubiquitous *tsen54* expression observed as early as the 8-cell stage is compatible with an essential function of this gene during development. Our data confirm results from previous studies in zebrafish embryos using *tsen54* RNA probes (24). Importantly, a comparable *TSEN54* expression pattern is observed in humans and zebrafish during early neurodevelopmental stages.

Although obvious anatomical differences exist between the species, comparisons can be made between the brain phenotypes observed in *tsen54* morphant zebrafish embryos and *TSEN54*-related PCH. The presence of progressive microcephaly and cortical shrinkage is a distinctive pathology associated with a PCH2 phenotype (1). Therefore, the observation of brain hypoplasia in zebrafish embryos following *tsen54* knockdown is an expected phenotype. A general neurodevelopmental delay and immaturation of the brain is also associated with the disease (1). PCH is considered a neurodevelopmental, neurodegenerative disorder, however, in contrast to other neurodevelopmental disorders such as lissencephaly (27), a brain patterning defect is not associated with PCH. Here, we tested for neurodevelopmental abnormalities in our *tsen54* MO knockdown model by monitoring the expression

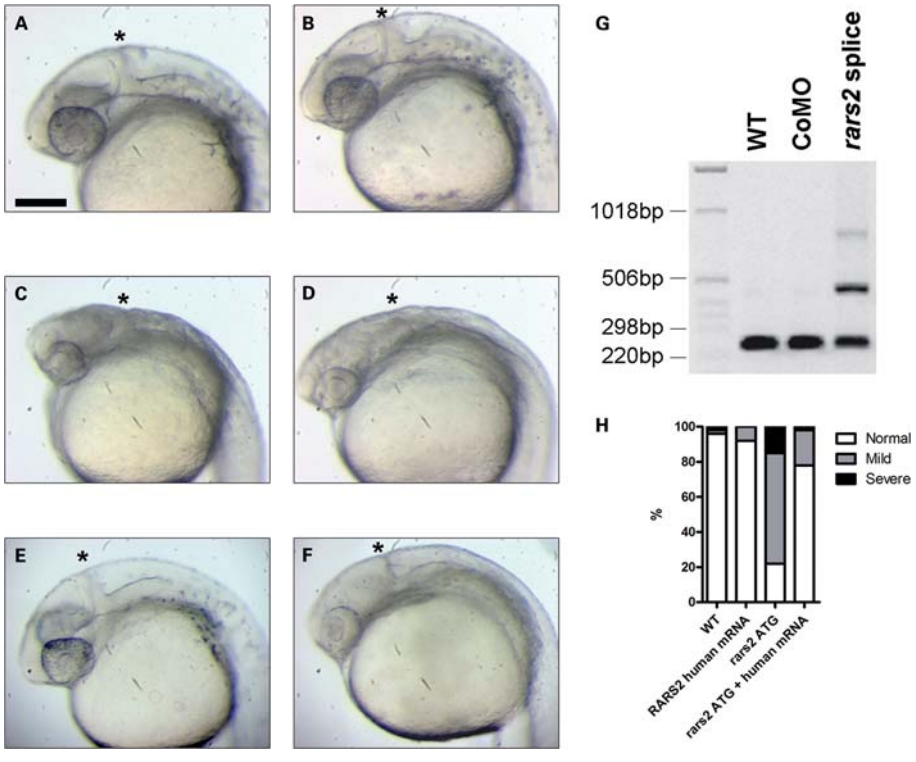

Figure 6. Disruption of *rars2* gene results in brain phenotype comparable with *tsen54* knockdown. (**A**–**F**) Head and brain regions of *rars2* MO and human *RARS2* mRNA-injected zebrafish embryos at 24 hpf. Asterisks denote the MHB. (A) WT un-injected embryo; (B) CoMO-injected embryo; (C) *rars2* ATG MO-injected embryo; (D) *rars2* exon 6 splice donor site MO-injected embryo; (E) human *RARS2* mRNA-injected embryo; (F) rescued embryo co-injected with *rars2* ATG MO and human *RARS2* mRNA. Scale bar = 200 μm. (**G**) RT–PCR using primers located in exons 3 and 6 in *rars2* cDNA synthesized from RNA extractions from WT un-injected embryos, CoMO-injected embryos and *rars2* exon 6 splice donor site MO-injected embryos. RT–PCR using samples from control embryos produced a band of 246 bp in length. Larger products observed in splice MO-injected embryos indicate abnormal splicing of the *rars2* gene. (**H**) Quantification of phenotypes observed in WT un-injected embryos, human *RARS2* mRNA-injected embryos, *rars2* ATG MO-injected embryos and rescued embryos co-injected with ATG MO and human mRNA. For each group, 50–100 embryos were analysed. Embryos were classified as displaying normal (white), mild (grey) or severe (black) phenotypes. There is a shift from a predominantly mild-severe phenotype in the *rars2* ATG MO group to a predominantly normal phenotype in ATG MO and human *RARS2* mRNA co-injection group, thus illustrating the partial rescue of the brain phenotype associated with the loss of *rars2*.

of *Fgf8* and *Otx2*. Expression of these genes was observed within the appropriate regions for this developmental stage thus indicating that a brain patterning deficiency was not associated with a loss of *tsen54*. Low levels of cell death within the pons have been reported in few PCH patients (5). However, as PCH is a neurodegenerative disorder occurring during early brain development, it is likely that high levels of cell death occur during earlier time points of the disease, rendering these cells unavailable for post-mortem analysis. Indeed, a significant increase in the number of acridine orange fluorescing cells was evident in the brains of *tsen54* morphants. Therefore, these data suggest that the brain phenotype caused by the loss of *tsen54* function is due to an increased activation of processes leading to cell death and neurodegeneration. It should be noted that not all tissues with high expression of *TSEN54* are affected in PCH patients. Since we show here that PCH is in fact a neurodegenerative disease and not a developmental defect *per se*, other factors must determine the tissue-specific defect. A possible explanation could be a large demand for specific tRNAs for protein synthesis during a specific time in development. As discussed in more detail below, if this demand is not met, cells may degenerate.

The majority of *TSEN54*-related PCH patients die within the first decade of life (1). In the most severe cases, a *TSEN54* null allele occurring compound heterozygous with the common p.A307S mutation can lead to early post-natal death (1,2). We identified the *tsen54*^{R228X} ENU mutation and as expected heterozygous mutants were viable. It is likely that possessing two copies of a premature stop-codon mutation leads to a non-functional or absent protein; thus, we predicted that the loss of *tsen54* would be lethal. To date, no patients have been identified that harbour homozygous premature stop-codon mutations in *TSEN54*. Due to the potential severity of this type of mutation, it is possible that these patients never survive through prenatal stages. A *tsen54*$^{R228X+/-}$ in-cross produced the expected mendelian ratios (observed following genotyping at 5 dpf), however by 9 dpf, all *tsen54*$^{R228X-/-}$ larvae had died. In comparison, 45% of *tsen54*$^{R228X+/+}$ and 62% of *tsen54*$^{R228X+/-}$ survived beyond the 21 dpf time-point. These data therefore strongly suggest that homozygosity of the *tsen54* premature stop-codon mutation is larval lethal in this model. The absence of a brain phenotype (data not shown) and the survival up to 9 dpf in the *tsen54*$^{R228X-/-}$ mutants may be explained by the persistence of maternal *tsen54*

protein during embryogenesis (28). Extensive characterization of the *tsen54*$^{R228X-/-}$ mutant line is necessary to fully establish this model as a tool to study the disease mechanisms underlying *TSEN54*-related PCH.

In both human and zebrafish, the loss of *TSEN54/tsen54* function results in a severe region-specific neurological phenotype. Due to the primary function of the TSEN complex, these observations therefore suggest that a high level of tRNA-splicing activity is required within these brain regions during development. Demand for such activity suggests that there is a larger proportion of intron-containing tRNA genes expressed within these regions. Intron-containing tRNA genes are rare in vertebrates (only 6.2% in humans); therefore, tRNA-splicing activity is only required for a small proportion of tRNA genes. However, reduced tRNA-splicing activity may still lead to a reduction in the availability of specific tRNAs, e.g. tRNA tyrosine, where 13 of the 14 tRNA^{Tyr}-(GTA) genes contain an intron. In zebrafish, there is ~20-fold more tRNA genes present in comparison to human; however, intron-containing tRNA genes still only represent 6.6% of the total (http://lowelab.ucsc.edu/GtRNAdb/). As in humans, the vast majority of zebrafish tRNA^{Tyr}-(GTA) genes contain an intron (225 out of 236). Hypothetically, therefore, it is reasonable to suggest that in both species, the loss of tRNA-splicing function could lead to a reduction in the availability of tRNA^{Tyr}. If the expression levels of intron-containing tRNA genes are higher in specific brain structures, then a depletion of tyrosine and/or other amino acids could explain the brain-specific degeneration observed in *TSEN54*-related PCH and the zebrafish *tsen54* knockdown model. Due to extensive secondary and tertiary structures, little is known about the spatio-temporal expression levels of different tRNA genes. However, one study has revealed that the expression levels of different human tRNA genes vary greatly between tissues that may reflect translational control based on the availability of certain tRNAs (29). Future experiments may benefit from examining the levels of intron-containing tRNA genes within the cerebellum and pons in comparison to other tissues. An alternative suggestion for specific susceptibility of the cerebellum and pons in the pathogenesis of PCH may relate to an alternative function of TSEN. For example, the human TSEN complex has been shown to associate with factors involved with pre-mRNA 3′ end formation (7). Therefore, it is feasible that this and/or other currently unknown functions relating to RNA processing may exist for TSEN.

As the *RARS2* gene plays a role in the aminoacylation of mitochondrial tRNA^{Arg} (4) and mutations in this gene are found in PCH1 and PCH6 (1,4,13), we tested whether the knockdown of *rars2* in zebrafish resulted in a similar phenotype to *tsen54* inhibition. Comparable phenotypes were observed between the *rars2* and *tsen54* groups. The obvious functional link between *TSEN54* and *RARS2* is an involvement with tRNA processing. Although specific phenotypical differences exist between *TSEN54*- and *RARS2*-related PCH, all patients display hypoplasia and variable atrophy of the cerebellum and pons. The comparable brain phenotype observed following *tsen54* and *rars2* knockdown therefore provides evidence in a model system that a common disease pathway may exist between PCH subtypes. As for *TSEN54*, aminoacyl tRNA synthetases (ARSs) are also expressed ubiquitously in humans (30). In zebrafish at 24 hpf, *rars2* is ubiquitously expressed; however, strongest expression is observed within the brain (24). Mutations in various cytoplasmic and mitochondrial ARS genes have been identified in leukoencephalopathy (DARS2) (31) and different subtypes of Charcot-Marie-Tooth disease [GARS (32), YARS (33), KARS (34)]. Recently, mutations in *SEPSECS*, a protein involved with the synthesis of the amino acid selenocysteine, have been reported to cause progressive cerebello-cerebral atrophy, a neurodevelopmental disorder with comparable phenotypic features to PCH (35). Taken together with our data, these studies suggest different neuronal populations at different stages of life are susceptible to disruption of specific amino acid availability. Defects in tRNA splicing and tRNA aminoacylation caused by the loss of *TSEN54* and *RARS2* function, respectively, may ultimately reduce the availability of functionally charged tRNA. Therefore, a common disease pathway involving *TSEN54* and *RARS2* may relate to the abnormal processing of cytoplasmic and mitochondrial tRNAs within the brain. We cannot yet, however, rule out the potential for alternative functions of these genes in the pathogenesis of PCH. Nevertheless, the identification of a mutation in *MED17* (36), encoding a subunit of the mediator complex involved with transcription pre-initiation, in patients with cerebral and cerebellar atrophy (CCA) supports the hypothesis that an unmet demand for protein synthesis at a specific moment in development is the underlying cause of cerebellar atrophy or hypoplasia in CCA and PCH.

MATERIALS AND METHODS

Zebrafish stocks and maintenance

All zebrafish (*Danio rerio*) procedures were approved by the Academic Medical Center Animal Ethics Committee and experiments complied with standard animal care guidelines. Breeding and maintenance of all zebrafish stocks was performed as described by others (37). WT TL zebrafish strains were crossed to generate embryos for MO and RNA injections, as well as *in situ* hybridizations. ENU mutant zebrafish lines were maintained on a mixed AB/TL background. Fertilized embryos were collected and staged according to the standard guidelines (38).

In situ hybridization using LNA–2OME-modified oligonucleotides to detect *TSEN54* expression in human fetal sections

Human embryonic tissue was collected and prepared for histological analyses as described (39). Use of the human embryos for research was approved by the Ethical Committee of the University of Amsterdam, the Netherlands. Pre-hybridization conditioning and hybridization using a human *TSEN54* specific, fluorescein-labelled LNA/2OME probe (5′-TcuTuc TcuTgcCauCucC-3′; where LNA residues are given in capital letters and 2OME in lower case) was performed as described previously (2). Probes were synthesized by Ribotask ApS, Odense, Denmark. Hybridization signal was detected by incubating the sections in blocking buffer containing anti-fluorescein-Alkaline phosphatase (AP) Fab fragments

(1:1000; Roche, Lewes, UK) for 1 h at room temperature. AP signal was detected by using VECTOR Blue AP Substrate Kit (Vector, Burlingame, CA, USA).

Zebrafish whole-mount *in situ* hybridization using LNA/2OME probes

Embryos were dechorionated, fixed in 4% paraformaldehyde (PFA) in 0.1% phosphate buffered saline-Tween (PBST) and stored in methanol at −20°C till further use. Prehybridization conditioning and hybridization using a zebrafish *tsen54* specific, fluorescein-labelled LNA/2OME probe (5′-TauCugTccCgcTccCucT-3′; Ribotask ApS) was performed on whole embryos as described by others (40). Hybridization signal was detected by incubating the embryos in blocking buffer containing anti-fluorescein-AP Fab fragments (1:2000; Roche) with agitation overnight at 4°C. AP staining was performed using 5-bromo-4-chloro-3-indolyl phosphate/nitro blue tetrazolium substrate.

MO injections

MOs (Gene-tools, LLC, Philomath, OR, USA) were designed around the start codon (ATG) and the exon 8 splice donor site of the zebrafish *tsen54* gene (ATG: 5′-CTTGCCTCTTTCTG AAAAACCCATC-3′; Ex8splice: 5′-TAGTGTAAAGTACAT CTTACGGTGT-3′). For the zebrafish *rars2* gene, MOs were designed against the ATG and the exon 6 splice donor sequence (ATG: 5′-CACTCCTCCTGAAAAAACACGCCA T-3′; Ex6splice: 5′-CACACACACAGTAAACTGACCTG AA-3′). Standard CoMOs were also provided by Gene-tools. Using fine glass needles and a microinjector (World Precision Instruments, Sarasota, FL, USA), 1–4-cell stage embryos were injected directly into the yolk sac with 2.5 ng ATG MO, 3.2 ng splice MO or 6.6 ng CoMO. Embryos were allowed to recover in E3 medium stored at 28°C before fixation at various time points.

Human mRNA *in vitro* transcription and injections

Human *TSEN54* cDNA cloned into the pCMV-SPORT6 vector (NIH_MGC_71) and human *RARS2* cDNA cloned into the pOTB7 vector (NIH_MGC_44) were obtained from the Mammalian Gene Collection (NIH, Bethesda, USA). The *TSEN54* insert was excised using *Xho*I and *Eco*RI; the *RARS2* insert was excised using *Bam*HI and *Xho*I. Both cDNA sequences were ligated into separate pCS2+ vectors. The *TSEN54* and *RARS2* constructs were linearized with Asp718 and Not1, respectively, and *in vitro* transcription was performed using the SP6 mMESSAGE mMACHINE kit (Ambion, Warrington, UK). For injections, 233 or 555 pg of *TSEN54* and *RARS2* mRNA, respectively, was injected per embryo either alone as a control or in combination with the ATG MO. For each group, 50–100 embryos at 24 hpf were classified and counted as displaying phenotypes described as either normal (appeared as WT), mild (slightly smaller head, slightly reduced brain structure definition) or severe (small head, complete loss of brain structural definition).

RT–PCR

To confirm specific targeting of the splice MO, total RNA was extracted from 50 injected embryos using TRIzol (Invitrogen, Germany) and chloroform for phase separation and isopropanol precipitation. For the reverse transcription reaction, 1 μg of RNA was mixed with 125 pmol/μl OligodT_{12}-VN and denatured for 10 min at 72°C. First-strand cDNA was synthesized using SuperscriptII enzyme (Invitrogen) and incubating at 42°C for 1 h. For *tsen54* ex8 splice MO, a region of 696 bp spanning exons 7 and 10 was amplified using the following primers: 5′-CAGCATCGGACAAACAGAAG-3′ and 5′-ACTGGTCTGACGGGGACA-3′ (Sigma-Aldrich). For *rars2* ex6 splice MO, a region of 246 bp spanning exons 3 and 6 was amplified using the following primers: 5′-GAGACCTGCAGAACACCACA-3′ and 5′-AACTTCTT GGCGATGTTTGG-3′ (Sigma-Aldrich).

Whole-mount *in situ* hybridization using DIG-labelled RNA probes

fgf8 (18) and *otx2* (20) were linearized with *Eco*RV and *Eco*RI, respectively, and digoxigenin (DIG)-RNA probes were synthesized using the SP6/T7 polymerase RNA labelling kit (Roche). Zebrafish embryos (24–30 hpf) were dechorionated, fixed overnight at 4°C in 4% PFA in 0.1% PBST and stored in methanol at −20°C till further use. Whole-mount *in situ* hybridization was performed as described by others (41).

In vivo cell death assay

Live embryos were incubated for 30 min in the dark at 28°C in water containing 2 μg/ml acridine orange (Sigma-Aldrich). Embryos were washed five times in water prior to imaging. The numbers of fluorescing cells in focus were counted within the brain in a region encapsulating the tip of the forebrain to the ear. Dying cells within the eye were omitted from the analysis. Fluorescing cells were counted in 10–20 embryos/larvae per condition. The mean number of fluorescing cells ± standard error was plotted. One-way ANOVA with the Newman–Keuls multiple comparisons test was performed for statistical analysis.

ENU mutagenesis screen

ENU mutation screening was performed using a TILLING (targeting induced local lesions IN genomics) approach with a frozen archive of genomic DNA derived from mutagenized F1 zebrafish at the Hubrecht Institute, Utrecht, the Netherlands, as described previously (42). Exon 8 of the *tsen54* gene was amplified using the following nested PCR primers (Primer 1: 5′-GGGACTTCAGCAGCATTAG-3′; Primer 2: 5′-AGGAGATCTGAGCGTTTGG-3′; Primer 3: 5′-CCAGT CTTTACCCAGTCACC-3′; Primer 4: 5′-CTTCCAACAAT CTTTCTTTCC-3′; Sigma-Aldrich). The first PCR was performed using primers 1 and 4. The second PCR was performed using primers 2 and 3, which contained universal M13 forward (M13F) and M13 reverse (M13R) adaptor sequences at their 5′ ends, respectively. Mutation detection and verification was therefore performed by sequencing the internal nested PCR

product using M13F (5′-TGTAAAACGACGGCCAGT-3′; Sigma-Aldrich) and M13R primers (5′-AGGAAACAGCTAT GACCAT-3′; Sigma-Aldrich). PCR products were sequenced as described previously (1).

Taqman genotyping

Following identification of the individual heterozygous c.682C > T *tsen54* mutant (hu5985) in the live F1 library, the mutation was backcrossed onto a WT AB background for five generations to reduce the number of potentially confounding ENU mutations. For each subsequent generation, genotyping was performed using a Taqman single-nucleotide polymorphism (SNP) genotyping approach (Applied Biosystems, Warrington, UK). Briefly, fish were anaesthetized in 250 mg/l tricaine (MS-222; Sigma-Aldrich), and a small portion of the caudal fin was removed with a scalpel. Fin clips were digested with lysis buffer containing 0.1 mg/ml of proteinase K at 60°C for 1 h. Following DNA quantification, 10 ng of DNA was added to 1 × 5 μl of Roche Fast-Start universal probe mix (Roche) containing 40× Taqman SNP assay probe (designed and generated by Applied Biosystems; FAM and VIC dye-labelled). Real-time PCR was then performed using a Roche LightCycler 480 for 40 cycles (denatured at 95°C for 15 s, annealed/amplified at 60°C for 1 min). Allelic discrimination was analysed using the Roche LightCycler software version 1.5.

Survival analysis in *tsen54*^{R228X} mutant zebrafish

Progenies from an in-cross mating of *tsen54*$^{R228X+/-}$ adults were raised for 3 weeks. Dead larvae were removed from the tank twice daily and DNA was extracted immediately before freezing. At 21 dpf, all surviving larvae were humanely sacrificed and DNA was extracted. All dead and surviving embryos were genotyped as described above. Survival of *tsen54*$^{R228X-/-}$ larvae was examined using the Kaplan–Meier analysis (Graphpad Prism, version 5) to produce survival curves for each genotype. Similarly, progenies from an in-cross mating of WT TL adults were raised for 3 weeks and dead larvae were counted on a daily basis for survival analysis.

SUPPLEMENTARY MATERIAL

Supplementary Material is available at *HMG* online.

ACKNOWLEDGEMENTS

We would like to thank C. van Rooijen and W. de Graaf for technical assistance with zebrafish maintenance and M. Brand and E. Weinberg for providing RNA probes. We would also like to thank E. Cuppen and H. van Roekel for support with ENU TILLING.

Conflict of Interest statement. None declared.

FUNDING

We would like to thank ZF Health for funding the ENU TILLING library and support by the 'Internationale Stichting Alzheimer Onderzoek' (ISAO #07508 and #09506) to P.T. and D.Z. Y.N. is supported by an AMC graduate school fellowship.

REFERENCES

1. Namavar, Y., Barth, P.G., Kasher, P.R., van Ruissen, F., Brockmann, K., Bernert, G., Writzl, K., Ventura, K., Cheng, E.Y., Ferriero, D.M. *et al.* (2011) Clinical, neuroradiological and genetic findings in pontocerebellar hypoplasia. *Brain*, **134**, 143–156.
2. Budde, B.S., Namavar, Y., Barth, P.G., Poll-The, B.T., Nurnberg, G., Becker, C., van Ruissen, F., Weterman, M.A., Fluiter, K., te Beek, E.T. *et al.* (2008) tRNA splicing endonuclease mutations cause pontocerebellar hypoplasia. *Nat. Genet.*, **40**, 1113–1118.
3. Durmaz, B., Wollnik, B., Cogulu, O., Li, Y., Tekgul, H., Hazan, F. and Ozkinay, F. (2009) Pontocerebellar hypoplasia type III (CLAM): extended phenotype and novel molecular findings. *J. Neurol.*, **256**, 416–419.
4. Edvardson, S., Shaag, A., Kolesnikova, O., Gomori, J.M., Tarassov, I., Einbinder, T., Saada, A. and Elpeleg, O. (2007) Deleterious mutation in the mitochondrial arginyl-transfer RNA synthetase gene is associated with pontocerebellar hypoplasia. *Am. J. Hum. Genet.*, **81**, 857–862.
5. Patel, M.S., Becker, L.E., Toi, A., Armstrong, D.L. and Chitayat, D. (2006) Severe, fetal-onset form of olivopontocerebellar hypoplasia in three sibs: PCH type 5? *Am. J. Med. Genet. A*, **140**, 594–603.
6. Renbaum, P., Kellerman, E., Jaron, R., Geiger, D., Segel, R., Lee, M., King, M.C. and Levy-Lahad, E. (2009) Spinal muscular atrophy with pontocerebellar hypoplasia is caused by a mutation in the VRK1 gene. *Am. J. Hum. Genet.*, **85**, 281–289.
7. Paushkin, S.V., Patel, M., Furia, B.S., Peltz, S.W. and Trotta, C.R. (2004) Identification of a human endonuclease complex reveals a link between tRNA splicing and pre-mRNA 3′ end formation. *Cell*, **117**, 311–321.
8. Trotta, C.R., Paushkin, S.V., Patel, M., Li, H. and Peltz, S.W. (2006) Cleavage of pre-tRNAs by the splicing endonuclease requires a composite active site. *Nature*, **441**, 375–377.
9. Hopper, A.K. and Phizicky, E.M. (2003) tRNA transfers to the limelight. *Genes Dev.*, **17**, 162–180.
10. Huang, H., Xue, R., Zhang, J., Ren, T., Richards, L.J., Yarowsky, P., Miller, M.I. and Mori, S. (2009) Anatomical characterization of human fetal brain development with diffusion tensor magnetic resonance imaging. *J. Neurosci.*, **29**, 4263–4273.
11. Graham, J.M. Jr., Spencer, A.H., Grinberg, I., Niesen, C.E., Platt, L.D., Maya, M., Namavar, Y., Baas, F. and Dobyns, W.B. (2010) Molecular and neuroimaging findings in pontocerebellar hypoplasia type 2 (PCH2): is prenatal diagnosis possible? *Am. J. Med. Genet. A*, **152A**, 2268–2276.
12. Bandmann, O. and Burton, E.A. (2010) Genetic zebrafish models of neurodegenerative diseases. *Neurobiol. Dis.*, **40**, 58–65.
13. Rankin, J., Brown, R., Dobyns, W.B., Harington, J., Patel, J., Quinn, M. and Brown, G. (2010) Pontocerebellar hypoplasia type 6: a British case with PEHO-like features. *Am. J. Med. Genet. A*, **152A**, 2079–2084.
14. Parisi, M.A. and Dobyns, W.B. (2003) Human malformations of the midbrain and hindbrain: review and proposed classification scheme. *Mol. Genet. Metab.*, **80**, 36–53.
15. Koster, R.W. and Fraser, S.E. (2001) Direct imaging of in vivo neuronal migration in the developing cerebellum. *Curr. Biol.*, **11**, 1858–1863.
16. Eisen, J.S. and Smith, J.C. (2008) Controlling morpholino experiments: don't stop making antisense. *Development*, **135**, 1735–1743.
17. Barth, P.G., Aronica, E., de Vries, L., Nikkels, P.G., Scheper, W., Hoozemans, J.J., Poll-The, B.T. and Troost, D. (2007) Pontocerebellar hypoplasia type 2: a neuropathological update. *Acta Neuropathol.*, **114**, 373–386.
18. Reifers, F., Bohli, H., Walsh, E.C., Crossley, P.H., Stainier, D.Y. and Brand, M. (1998) Fgf8 is mutated in zebrafish acerebellar (ace) mutants and is required for maintenance of midbrain-hindbrain boundary development and somitogenesis. *Development*, **125**, 2381–2395.
19. Picker, A. and Brand, M. (2005) Fgf signals from a novel signaling center determine axial patterning of the prospective neural retina. *Development*, **132**, 4951–4962.
20. Li, Y., Allende, M.L., Finkelstein, R. and Weinberg, E.S. (1994) Expression of two zebrafish orthodenticle-related genes in the embryonic brain. *Mech. Dev.*, **48**, 229–244.

21. van Ham, T.J., Mapes, J., Kokel, D. and Peterson, R.T. (2010) Live imaging of apoptotic cells in zebrafish. *FASEB J.*, **24**, 4336–4342.
22. de Bruijn, E., Cuppen, E. and Feitsma, H. (2009) Highly efficient ENU mutagenesis in zebrafish. *Methods Mol. Biol.*, **546**, 3–12.
23. Keays, D.A., Clark, T.G. and Flint, J. (2006) Estimating the number of coding mutations in genotypic- and phenotypic-driven N-ethyl-N-nitrosourea (ENU) screens. *Mamm. Genome*, **17**, 230–238.
24. Thisse, B. and Thisse, C. (2004) Fast release clones. A high throughput expression analysis. ZFIN direct data submission, http://zfin.org.
25. Sarnat, H.B., Benjamin, D.R., Siebert, J.R., Kletter, G.B. and Cheyette, S.R. (2002) Agenesis of the mesencephalon and metencephalon with cerebellar hypoplasia: putative mutation in the EN2 gene—report of 2 cases in early infancy. *Pediatr. Dev. Pathol.*, **5**, 54–68.
26. Xuan, S., Baptista, C.A., Balas, G., Tao, W., Soares, V.C. and Lai, E. (1995) Winged helix transcription factor BF-1 is essential for the development of the cerebral hemispheres. *Neuron*, **14**, 1141–1152.
27. Yamada, M., Yoshida, Y., Mori, D., Takitoh, T., Kengaku, M., Umeshima, H., Takao, K., Miyakawa, T., Sato, M., Sorimachi, H. *et al.* (2009) Inhibition of calpain increases LIS1 expression and partially rescues in vivo phenotypes in a mouse model of lissencephaly. *Nat. Med.*, **15**, 1202–1207.
28. Wagner, D.S., Dosch, R., Mintzer, K.A., Wiemelt, A.P. and Mullins, M.C. (2004) Maternal control of development at the midblastula transition and beyond: mutants from the zebrafish II. *Dev. Cell*, **6**, 781–790.
29. Dittmar, K.A., Goodenbour, J.M. and Pan, T. (2006) Tissue-specific differences in human transfer RNA expression. *PLoS Genet.*, **2**, e221.
30. Antonellis, A. and Green, E.D. (2008) The role of aminoacyl-tRNA synthetases in genetic diseases. *Annu. Rev. Genomics Hum. Genet.*, **9**, 87–107.
31. Scheper, G.C., van der Klok, T., van Andel, R.J., van Berkel, C.G., Sissler, M., Smet, J., Muravina, T.I., Serkov, S.V., Uziel, G., Bugiani, M. *et al.* (2007) Mitochondrial aspartyl-tRNA synthetase deficiency causes leukoencephalopathy with brain stem and spinal cord involvement and lactate elevation. *Nat. Genet.*, **39**, 534–539.
32. Antonellis, A., Ellsworth, R.E., Sambuughin, N., Puls, I., Abel, A., Lee-Lin, S.Q., Jordanova, A., Kremensky, I., Christodoulou, K., Middleton, L.T. *et al.* (2003) Glycyl tRNA synthetase mutations in Charcot-Marie-Tooth disease type 2D and distal spinal muscular atrophy type V. *Am. J. Hum. Genet.*, **72**, 1293–1299.
33. Jordanova, A., Irobi, J., Thomas, F.P., Van Dijck, P., Meerschaert, K., Dewil, M., Dierick, I., Jacobs, A., De Vriendt, E., Guergueltcheva, V. *et al.* (2006) Disrupted function and axonal distribution of mutant tyrosyl-tRNA synthetase in dominant intermediate Charcot-Marie-Tooth neuropathy. *Nat. Genet.*, **38**, 197–202.
34. McLaughlin, H.M., Sakaguchi, R., Liu, C., Igarashi, T., Pehlivan, D., Chu, K., Iyer, R., Cruz, P., Cherukuri, P.F., Hansen, N.F. *et al.* (2010) Compound heterozygosity for loss-of-function lysyl-tRNA synthetase mutations in a patient with peripheral neuropathy. *Am. J. Hum. Genet.*, **87**, 560–566.
35. Agamy, O., Ben, Z.B., Lev, D., Marcus, B., Fine, D., Su, D., Narkis, G., Ofir, R., Hoffmann, C., Leshinsky-Silver, E. *et al.* (2010) Mutations disrupting selenocysteine formation cause progressive cerebello-cerebral atrophy. *Am. J. Hum. Genet.*, **87**, 538–544.
36. Kaufmann, R., Straussberg, R., Mandel, H., Fattal-Valevski, A., Ben-Zeev, B., Naamati, A., Shaag, A., Zenvirt, S., Konen, O., Mimouni-Bloch, A. *et al.* (2010) Infantile cerebral and cerebellar atrophy is associated with a mutation in the MED17 subunit of the transcription preinitiation mediator complex. *Am. J. Hum. Genet.*, **87**, 667–670.
37. Klooster, J., Yazulla, S. and Kamermans, M. (2009) Ultrastructural analysis of the glutamatergic system in the outer plexiform layer of zebrafish retina. *J. Chem. Neuroanat.*, **37**, 254–265.
38. Kimmel, C.B., Ballard, W.W., Kimmel, S.R., Ullmann, B. and Schilling, T.F. (1995) Stages of embryonic development of the zebrafish. *Dev. Dyn.*, **203**, 253–310.
39. Sizarov, A., Anderson, R.H., Christoffels, V.M. and Moorman, A.F. (2010) Three-dimensional and molecular analysis of the venous pole of the developing human heart. *Circulation*, **122**, 798–807.
40. Kloosterman, W.P., Wienholds, E., de Bruijn, E., Kauppinen, S. and Plasterk, R.H. (2006) In situ detection of miRNAs in animal embryos using LNA-modified oligonucleotide probes. *Nat. Methods*, **3**, 27–29.
41. Thisse, C. and Thisse, B. (2008) High-resolution in situ hybridization to whole-mount zebrafish embryos. *Nat. Protoc.*, **3**, 59–69.
42. Wienholds, E., van Eeden, F., Kosters, M., Mudde, J., Plasterk, R.H. and Cuppen, E. (2003) Efficient target-selected mutagenesis in zebrafish. *Genome Res.*, **13**, 2700–2707.